International Journal of Bioelectromagnetism
Vol. 8, No. 1, pp. 31-43, 2006

www.ijbem.org

Estimation of Cortical Activity and Connectivity Related to Memory Tasks by High Resolution EEG recordings

Febo Cincotti[a], Fabio Babiloni[a,b], Donatella Mattia[a], and Laura Astolfi[a,b]

[a]*IRCCS "Fondazione Santa Lucia",Rome, Italy,*

[b]*Dep. of Human Physiology and Pharmacology, Univ. of Rome "La Sapienza", Rome, Italy*

Correspondence: Febo Cincotti, IRCCS "Fondazione Santa Lucia", Rome, Italy, via Ardeatina 306, 00100, Rome, Italy
E-mail: *febo.cincotti@uniroma1.it*, phone +39 06 51501466

Abstract. In this study, we presented a methodology useful to estimate statistically significant distributed sources of cortical activity by using non-invasive high-resolution electroencephalography (HREEG) recordings. Such methodology was demonstrated on HREEG data gathered during different memory experiments in a group of healthy subjects. Cortical distributed sources were estimated by using as volume conductor model subjects' realistic magnetic resonance (MR)-constructed head models. To increase the reliability of the source estimations, an average of the current density estimates were performed in particular regions of interest (ROIs). Such ROIs were drawn on the cortical mantle in agreement with the known location of the Broadmann areas (BAs). By using an estimate of the HREEG noise standard deviation of the cortical current density over the different BAs it is possible to derive a gaussian estimator (z score) of the power spectra variations relative to the task analysed in selected frequency bands (Statistical Parametric Mapping; SPM). Moreover, due to statistical properties of the z score it is also possible to evaluate significant differences between the power spectra variations over BAs between different experimental tasks. Furthermore, functional connectivity estimates from the cortical waveforms in the experimental tasks were obtained with the use of Directed Transfer Function. Results obtained showed active participation of cortical prefrontal and parietal areas during the task phase in which an image has to be held in the memory before an appropriate decision has to be made by the subjects. Such information is not visible by using conventional mapping procedures. The presented methodology allows separating statistical significant current density estimates from the random fluctuations due to the noise in selected ROIs coincident with BAs.

Keywords: Significance Probability Mapping; Distributed current density estimates; Brodmann areas; inverse problem; high-resolution EEG, Functional connectivity

1. Introduction

It is well known that high-resolution EEG (HREEG) recording technique presents a very good temporal resolution (ms scale) and a moderate spatial resolution (in the order of 2-3 cm). The spatio-temporal resolution of HREEG is adequate to follow the complex temporal dynamics of brain phenomena [Nunez,1995]. Furthermore, the wide availability of magnetic resonance images of subjects' heads has made possible the use of realistic models for the head and the cortical surface in procedures involving the estimation of cortical current activity. It has been demonstrated that the use of realistic head models increases the accuracy of the cortical current reconstruction from HREEG data. Point-like models of cortical sources (such as the current dipole) are largely used in the analysis of primary evoked potentials/fields or epileptic spikes [Torquati et al., 2002; Stenbacka et al., 2002; Otsubo et al., 2001], However, such source models insufficiently represent extended cortical activations due to cerebral engagement in motor or cognitive tasks [Anourova et al., 2001; Okada et al., 1998]. In the distributed source approach, thousands of equivalent current dipoles covering the cortical surface modeled have been used, their strengths estimated by using linear and non-linear inverse procedures

[Dale et al., 1993; Phillips et al., 1997; Baillet et al., 1997; Baillet et al., 1999 Uutela et al., 1999]. The solution space (i.e., the set of all possible combinations of the cortical dipoles strengths) is generally reduced by using geometrical constraints. For example, the dipoles can be disposed along the reconstruction of cortical surface with a direction perpendicular to the local surface. An additional constraint involves forcing the dipoles to explain the recorded data with a minimum or a low amount of energy (minimum-norm solutions; [Dale et al., 1993]). However, a statistical characterization of the estimated cortical current densities is also needed, to understand if the observed changes in brain activity are due to chance alone or are induced by the experimental task. However, in the study of cognitive processes with EEG recordings frequency-related instead temporal analysis are often used [Pfurtscheller et al., 1999]. This because many cognitive processes produced marked variations of EEG spectral contents while the temporal variations of the electromagnetic field could be less informative, due to the jitter of the time components of the event-related potentials/fields [Klimesch et al., 1999]. Hence, an interest arose about the extension of the SPM approach to the analysis of EEG data computed in the frequency domain. Another aspect of interest for a possible extension of the SPM techniques to the frequency domain is related to the fact that often the experimental design requires that the same group of subjects performs different tasks. This occurs when cognitive paradigm like GO/NOGO or working/no working memory are investigated [Fallgatter et al., 1999; Bokura et al.,2001; Gevins et al., 1997; Gevins et al., 1998]. The comparison between these different tasks in the framework of SPM can be conveniently addressed by using the same approach used by the neuroscientific community for the fMRI studies. In fact, by using the properties of the z score, it is possible to derive a contrast technique that extends in the frequency domain the comparisons usually employed by the SPM between the task and the baseline periods.

Besides the statistical characterization of the cortical source activity from EEG recordings with the SPM, it is also of interest in the assessment of the functional connections existing between the cortical areas. In fact, the estimation of cortical connectivity is of paramount importance in order to infer the circuits and the temporal and functional relations between them during the examined task. Several techniques have been proposed for the study of functional brain connectivity with hemodynamic and electromagnetic measurements [Buchel and Friston, 1997; Lee et al., 2003; Brovelli et al., 2004]. Two main definitions of brain connectivity have been proposed along these years: functional and effective connectivity [Horwitz, 2003]. While functional connectivity is defined as the temporal correlation between spatially remote neurophysiologic events, the effective connectivity is defined as the simplest brain circuit which would produce the same temporal relationship as observed experimentally between cortical sites. As for the functional connectivity, the computational methods proposed to estimate how different brain areas are working together typically involve the estimation of some covariance properties between the different time series measured from the different spatial sites during motor and cognitive tasks studied by EEG and fMRI techniques. Structural Equation Modeling (SEM) is a technique that has been used for a decade to assess effective connectivity between cortical areas in humans by using hemodynamic and metabolic measurements [McIntosh and Lima, 1994; Buchel and Friston, 1997]. The basic idea of SEM differs from the usual statistical approach of modeling individual observations since SEM considers the covariance structure of the data. However, the estimation of cortical effective connectivity obtained with the application of the SEM technique on fMRI data has a low temporal resolution (in the order of several seconds) which is far from the time scale at which the brain operates normally. Such temporal resolution can be improved by applying the SEM to high-resolution EEG data [Astolfi et al., 2005a]. It is worth noticing that the SEM approach is model dependent, while in general, a connectivity model is not available before the data analysis. From this point of view, there is an interest in the functional connectivity methods that do not need an a priori connectivity model, since they are data-driven. Among the linear and non linear methods used to estimate functional brain connectivity [Nunez, 1995; Clifford Carter 1987, Gevins et al. 1989; Urbano et al., 1998; Inouye et al. 1995; Stam et al., 2002; Stam et al., 2003, Tononi et al., 1994], the frequency-based methods are particularly attractive for the analysis of EEG or MEG data, since the activity of neural populations is often best expressed in this domain [Pfurtscheller and Lopes da Silva, 1999; Gross et al., 2001, 2003]. Recently, it has been proposed the use of Directed Transfer Function (DTF) techniques for the estimation of functional connectivity between estimated cortical waveforms from high-resolution EEG data [Babiloni et al., 2005; Astolfi et al., 2005b]. The good quality of the estimation of such functional connectivity by the application of DTF has been tested by simulations [Astolfi et al., 2005b].

In this paper, we present a methodological approach that allows the use of spectral data in the framework of the SPM for the analysis of complex behavioral memory tasks. Furthermore, we showed the possibility of the application of DTF techniques to the estimated cortical activity from the gathered neuroelectric data in order to estimate functional connectivity patterns during the analyzed tasks. An application of the proposed approach is provided on data related a Short-Term Memory (STM) and No Short-Term memory (NSTM) paradigm and data related to a long-term memory experiment on the encoding (ENC) and delayed (RET) retrieval of images. Results obtained with the proposed technology showed active participation of cortical prefrontal and parietal areas during the task phase in which an image has to be held in the memory by the subjects. Such participation was not visible by using previously adopted conventional mapping procedures while was highlighted by the proposed statistical approach.

2. Material and Methods

2.1. Experimental Tasks

For the EEG recordings, the subjects were seated in a comfortable reclining armchair placed in a dimly-lit, sound-damped, and electrically-shielded room (magnetically insulated room). They kept their forearms resting on armchairs, with right index finger resting between two buttons spaced 6 cm each other. A computer monitor was placed in front of the subjects (about 100 cm). Subjects are exposed to the vision of a cue visual stimulus on the computer screen. Two types of tasks were investigated: one related to the short-term memory (in terms of seconds), the other related to the long-term memory (in terms of hours).

Short-Term Memory task. In the short-term memory condition (STM) these stimulus consists of a couple of vertical bar that were first presented (trigger time) and then hidden for few seconds (delay time) in the Short-Term Memory (STM) condition, while in the No Short-Term Memory (NSTM) condition the vertical bars remained on the screen. Hence, only during the STM task subjects were asked to hold the images in memory (delay period). In both STM and NSTM tasks, when the go stimulus appears on the computer screen, subjects were asked to produce a motor performance in accordance with the image. In particular, the subjects have to push the left button if the left bar on the screen is higher than the right vertical bar, or vice-versa. Brief on-line feedback on the performance was automatically provided. The timing of the STM task was the following: pre-trigger time with a duration of 1 sec; warning visual stimulus (trigger time) with a duration of 1 sec; the cue stimulus with a duration of 5.5-7.5 sec; the visual go stimulus with a duration of 1 sec and finally the inter-trial interval: duration 5 sec. The control condition in which the spatial bar remains on the screen for all the task duration will also be developed and this was called in the following no short-term memory condition (NSTM). The experiment included two trial blocks for the NSTM task and two trial blocks for the STM task (each block including 50 trials). The NSTM and STM blocks were intermingled according to a predefined sequence (pseudorandom order). The inter-block interval was of about 2 min. Subjects were told in advance if the block comprised NSTM or STM trials. Before the recording session, a training of about ten minutes familiarized subjects with the experimental apparatus and NSTM-STM tasks. Subjects were free to use any memorization strategy including “visuo-spatial imagery”, somato-motor preparation and covert verbal coding and rehearsal. Fig. 1 presents the typical images used to present the task to the experimental subjects for both the NSTM and STM tasks.

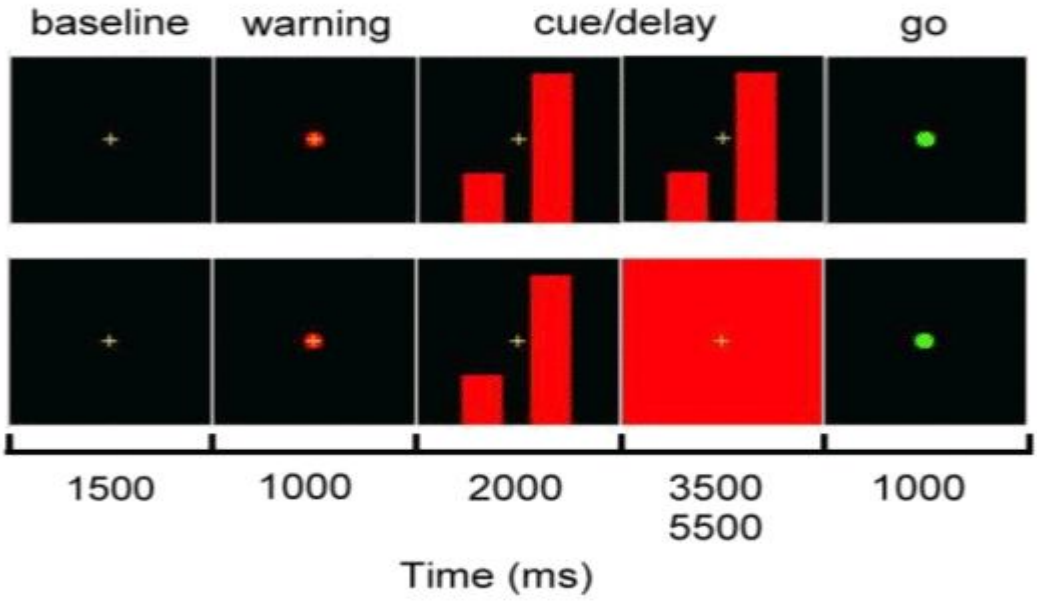

Figure 1. The experiment included a short-term memory (STM) task compared with a control no short-term memory (NSTM) task. The first row from the top presents the sequence of events for the STM condition. The second row presents the sequence of events for the NSTM condition. In the Short-Term Memory (STM) task the events are as follows: (1) a cross at the center of the monitor as baseline lasting 1 s; (2) a cross surrounded by a red circle at the center of the monitor as a visual warning stimulus lasting 1 s; (3) a couple of vertical bars as a visual cue stimulus lasting 2 s; (4) a blank screen as a delay period lasting 3.5–5.5 s; (5) a green circle at the center of the monitor as a go stimulus lasting 1 s; and (6) a finger movement as a motor response. Subjects had to click the left mouse button if the taller bar was at the left monitor side, or the right mouse button if the taller bar was at the right monitor side. Compared with the STM task, the NSTM task had visual cue stimuli lasting up to the go stimulus. The zero time was the onset of the cue stimulus.

Encoding and Retrieval tasks. In the long-term experiment there was an encoding (ENC) and a retrieval (RET) phase in which 50 complex colored magazine pictures were shown after a red central target given as a visual warning stimulus (presentation time of 1 s). In the ENC condition, 25 figures representing interiors of apartments ("indoor") were randomly intermingled with 25 figures representing landscapes ("landscapes"). The figures were shown one-by-one (cue period, the presentation time of 5 s). Subjects were instructed to press with right index finger one of the two buttons (left = "indoor"; right = "landscapes") as quickly as possible after the appearance of a green central target at the center of the figure (go stimulus, the presentation time of 1 s). Remarkably, no mention to a "retrieval" phase was made before the encoding phase, according to a standard paradigm of "incidental memory". About 1 hour later, the RET condition started. In this phase, 25 figures representing previously presented "indoor" ("tests") were randomly intermingled with 25 figures representing a novel "indoor" ("distractors"). Subjects were asked to discriminate between "tests" and "distractors" by pressing with right index finger one of the two buttons (left ="tests"; right = "distractors") immediately after the go stimulus. The timing of the warning stimulus, cue stimulus (picture presentation) and go stimulus were as in the "encoding" phase. Before the ENC phase, a training of about ten minutes was performed with a different set of figures to made familiar subjects with the experimental apparatus and general procedure used for the ENC-RET tasks, namely to press the mouse buttons with the right index finger after visual stimuli. Figure 2 presents the typical images used to present the task of encoding and retrieval to the experimental subjects.

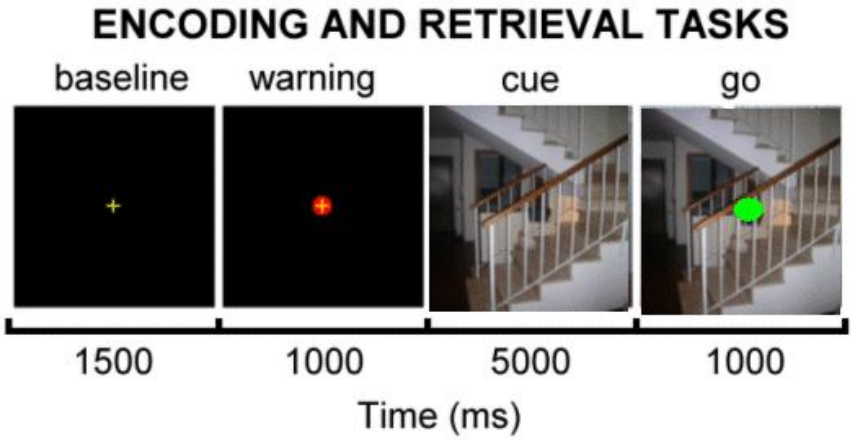

Figure 2. Set up and experimental tasks. The experiment included an "encoding" (ENC) and a "retrieval" (RET) tasks in which 50 complex colored magazine pictures were shown after a red central target given as a visual warning stimulus (presentation time of 1 s). In the ENC condition, 25 figures representing interiors of apartments ("indoor") were randomly intermingled with 25 figures representing landscapes ("landscapes"). The figures were shown one-by-one (cue period, the presentation time of 5 s). Subjects were instructed to press with right index finger one of the two close buttons (left = "indoor"; right = "landscapes") as quickly as possible after the appearance of a green central target at the center of the figure (go stimulus, the presentation time of 1 s). About 1 h later, the RET condition started. In this phase, 25 figures representing previously presented "indoor" ("tests") were randomly intermingled with 25 figures representing novel "indoor" ("distractors"). Subjects were asked to discriminate between "tests" among "distractors" by pressing one of the two buttons (left = "tests"; right = "distractors") immediately after the go stimulus. The timing of warning stimulus, cue stimulus (picture presentation) and go stimulus was as in the "encoding" phase.

2.2. Subjects and EEG recordings.

All the subjects involved in EEG experiments gave their informed written consent according to the Helsinki declaration. General recording procedures were approved by the local institutional ethics committees. Nine healthy subjects were considered in this study. Each EEG recording was made by using forty-six scalp electrodes, that were positioned according to an extension of the international 10-20 system extension. EEG data were recorded with 0.3-70 Hz bandpass and linked-earlobes reference. Electrooculogram (0.3-70 Hz bandpass) and surface rectified electromyographic activity of bilateral extensor digitorum muscles (1-70 Hz bandpass) were also collected. Artifact-free EEG activity from 3,5 s before to 4 s after the onset of the visual go stimulus (zerotime) was then considered for the EEG linear inverse procedures. EEG segments contaminated by blinking, eye movements, mirror movements and/or other artifacts were rejected off-line. In EEG recordings, frequency bands of interest were theta, alpha 1, alpha 2, and alpha 3 whose band limits were computed according to a standard procedure based on the peak of individual alpha frequency (IAF; [Klimesch et al., 1999]). IAF was defined as the frequency showing maximum power density peak within a large frequency range lasting from 4 to 14 Hz. It was calculated at baseline period (1-second epoch preceding the onset of the warning stimulus, –2000 to –1000 ms). With respect to IAF, these frequency bands were defined as follows: (i) theta as the IAF-7 Hz to IAF-4 Hz; (ii) alpha 1 or "lower-1 alpha band" as the IAF-4 Hz to IAF-2 Hz, (iii) alpha 2 or "lower-2 alpha band" as IAF-2 Hz to IAF, and (iv) alpha 3 or "upper alpha" as IAF to IAF+2 Hz. The power spectrum analysis was based on a FFT approach using Welch technique and Hanning

windowing function. To quantify the event-related percentage reduction of alpha oscillations, we followed the widely-used procedure for the computation of event-related desynchronization/synchronization (ERD/ERS>; [Pfuntscheller et al., 1999; Pfuntscheller et al., 1977]). The ERD/ERS was computed for theta, alpha 1, alpha 2 and alpha 3 bands, based on the individual determination of the IAF.

2.3. Cortical source estimation.

In this study, magnetic resonance (MR)-constructed subjects' realistic head models and an averaged one were used to compute individual cortical current density estimates and to visualize population data, respectively.. The averaged head model was constructed using a set of averaged MRIs of 152 normal subjects coming from the Montreal Neurological Institute. Scalp, skull, dura mater and cortical surfaces of the realistic and averaged head models were obtained with segmentation and contouring algorithms. The surfaces of the realistic head models were then used to build the Boundary Element Model of the head as volume conductor employed in the present study. A cortical surface reconstruction was accomplished with a tessellation of about 3,000 triangles. A current dipole was placed at the center of each triangle. The orientation of each dipole was placed perpendicular to the triangle surface, to model the alignment of the cortical neurons with respect to the cerebral cortex surface. Fig 1 presents the averaged head model adopted for the visualization of the population data in this paper.

When the EEG activity is mainly generated by circumscribed cortical sources (i.e. short-latency evoked potentials/magnetic fields), the location and strength of these sources can be reliably estimated by the dipole localization technique [Scherg et al., 1984; Salmelin et al., 1995]. In contrast, when EEG activity is generated by extended cortical sources (i.e. event-related potentials/magnetic fields), the underlying cortical sources can be described by using a distributed source model with spherical or realistic head models [Dale et al., 1993; Grave de Peralta et al., 1998; Pascual-Marqui, 1995]. With this approach, typically thousands of equivalent current dipoles covering the cortical surface modeled and located at the triangle center were used, and their strength was estimated by using linear and non-linear inverse procedures [Dale et al., 1993; Uutela et al., 1999]. Taking into account the measurement noise **n**, supposed to be normally distributed, an estimate of the dipole source density magnitudes **x**, that generated a measured potential **b** at a particular time instant t can be obtained by solving the linear system:

$$\mathbf{Ax} + \mathbf{n} = \mathbf{b} \qquad (1)$$

where A is a *m´n* matrix with number of rows equal to the number of sensors and number of columns equal to the number of modeled sources. We denote with $\mathbf{A}_{\times j}$ the potential distribution over the m sensors due to each unitary j-th cortical dipole. The collection of all the *m*-dimensional vectors $\mathbf{A}_{\times j}$, (j = 1,…, *n*) describes how each dipole generates the potential distribution over the head model, and this collection is called the lead field matrix **A**. This is a strongly under-determined linear system, in which the number of unknowns, dimension of the vector **x**, is greater than the number of measurements **b** of about one order of magnitude. The estimation of the current density vector **x** has been performed in this paper by using the weighted minimum norm solution [Grave de Peralta et al., 1998; Pascual-Marqui, 1995].

2.4. Spectral estimation of current densities.

According to the equation (1), let be **x**(t) the source estimates for each time instant t of the recorded event-related potentials/fields **b(**t). By computing the Fourier transform of the obtained solution **x**(t) we have

$$\mathbf{x}(t) = \mathbf{G}\bullet\mathbf{b}(t) \Rightarrow \mathbf{X}(f) = \mathbf{G}\bullet\mathbf{B}(f) \qquad (2)$$

where **X**(*f*), **B**(*f*) are the Fourier transform of the time-varying sources and potentials, respectively and **G** is the pseudoinverse matrix, that maps the recorded potentials **b** to the estimated current density vector **x**, To estimate the spectral contents of the obtained solutions **X**(f), the cross spectral density matrix **xCSD**(*f*) was computed according to the following formula, where the H indicates the Hermitian condition and the apex the transposition

$$\mathbf{xCSD}(f)=\mathbf{X}(f)'\mathbf{X}(f)^{\mathbf{H}} \qquad (3)$$

and from the positions above it follows

$$\mathbf{xCSD}(f)=\mathbf{G}\bullet\mathbf{B}(f)\bullet\mathbf{B}(f)^{\mathbf{H}}\bullet\mathbf{G}' = \mathbf{G}\bullet\mathbf{bCSD}(f)\bullet\mathbf{G}' \qquad (4)$$

where **bCSD**(*f*) is the spectral covariance matrix of the recorded data. The i-th entry of the xCSD(f) matrix ($\mathbf{xCSD_{ii}}(f)$) is relative to the power spectra of the i-th current dipole. After the spectral computations, the logarithmic transform was applied, to make the spectral data more gaussian than the untransformed ones.

2.5. The estimation of the cortical activity in the Regions of Interest

The estimation of the cortical activity returns a current density estimate for each one of the about 3,000 dipoles constituting the modeled cortical source space. Each dipole presents a time-varying magnitude representing the spectral power variations generated during the task time-course. This rather large amount of data can be synthesized by computing the ensemble average of all the dipoles magnitudes belonging to the same cortical region of interest (ROI). Each ROI was defined on the cortical model adopted in accordance with the Brodmann areas (BAs). Such areas are regions of the cerebral cortex whose neurons sharing the same anatomical (and often also functional) properties. One decades of neuroimaging studies assigned to different BAs a precise role in the reception and the analysis of sensory and motor commands, as well as the memory processing. Actually, such areas are largely used in neuroscience as a coordinate system for sharing cortical activation patterns found with different neuroimaging techniques. As a result of this anatomical-guided data reduction, we pass from the analysis of about 3,000 time series to the evaluation of less than one hundred, (the BAs located in both cerebral hemispheres). These BAs waveforms, related to the increase or decrease of the spectral power of the cortical current density in the investigated frequency band, can be successively averaged across the subjects of the studied population. The generated grand-average waveforms describe the time behavior of the spectral power increase or decrease of the current density in the population during the task examined.

2.6. Statistical significance of the estimated cortical activity

What is often missing in EEG linear inverse solutions is the level of reliability of the solution itself. Not all modelled sources have the same degree of sensitivity to measurement noise, so we cannot say whether a source has a high strength because it is the most probable source of that potential distribution, or just because that source well accounts for the noise superimposed to the potential. Even in the ideal case of absence of noise, some sources seem more inclined to explain a large set of data, just because of their geometrical properties (i.e. sources positioned on a cortical girus, rather than deep in a sulcus). A statistical approach to the problem and a measure of the signal to noise ratio in the modelled cortical activity are then required. The level of noise in the EEG linear inverse solutions can be addressed by estimating the "projection" of the EEG noise $\mathbf{n}(t)$ onto the cortical surface by means of the computed pseudoinverse operator $\mathbf{G}$; the standard error of the noise on the estimated source strength x_j is given by $\langle \mathbf{G}_j.\mathbf{n}(t) \rangle = \mathbf{G}_j.\mathbf{C}(\mathbf{G}_j.)'$, where $\mathbf{G}_j.$ is the j-th row of the pseudoinverse matrix, $\mathbf{C}$ is the EEG noise covariance matrix. This allows to quantitatively assess the ratio between the estimated cortical activity $\mathbf{x}$ and the amount of noise at the cortical level, quantified through the standard deviation of its estimate. It can be demonstrated that under the hypothesis of a normal estimate for the noise $\mathbf{n}(t)$ obtained with more than 50 time points, the following normally-distributed z score estimator can be obtained for each j-th cortical location and for each time point t considered

$$\mathbf{z}_j(t) = \frac{\mathbf{G}_{j.} \bullet \mathbf{b}(t)}{\sqrt{\left(\mathbf{G}_{j.}\,\mathbf{C}\,(\mathbf{G}_{j.})'\right)}} \tag{5}$$

where C is the estimated noise covariance matrix. The uncorrected threshold for the z score level at 5% is 1.96. Values of z exceeding such threshold represents levels of estimated cortical activity that are unlikely due to the chance alone but are related to the task performed by the experimental subject. However, to avoid the effects of the increase of the Type I error due to the multiple z tests performed, the results will be presented after the application of the Bonferroni correction [Zar, 1984].

Here, we extend the SPM approach to the analysis of the power spectra variations during the experimental task. The computation of the z score level in the spectral case is performed according to the following formula

$$\sigma^2 Noise_i = Var(bCSD_{ii}(f))$$

$$Z_i(f) = \frac{[G \bullet bCSD_{ii}(f) G']_i}{\sigma\, Noise_i} \tag{6}$$

where $Var(bCSD_{ii}(f))$ indicates the variance of the estimate of the log-transformed spectral density of the EEG measurements during the baseline period at the considered frequency f, and $Z_i(f)$ is the z score for the i-th current dipole for the frequency f. The $Z_i(f)$ it is for construction a z score variable, identical to those introduced in the time domain by Dale and colleagues [Dale et al., 2000], while the inverse operator G is identical to those computed for the temporal case.

The z score for each brain region investigated, independently as a result of a time or frequency domain processing, return information about the significance of the increase or the decrease of the variable considered in the analysed period with respect to the baseline chosen. Due to the additive properties of the z estimator, the z scores obtained for all the dipoles belong to a particular ROI can be averaged together. Furthermore, such average z scores for each particular ROI can be averaged across the subject's population, by returning a grand-average z score level for each ROI investigated. These values can be considered as an estimate of the statistical behaviour of the variable analyzed (in time or frequency domain) for the entire population in each one of the considered ROI.

In particular, the computation of the population z-score waveform for the *r*-th ROI while performing the *k*-th task is performed as follows:

$$z_{rk}^{(\text{grav})} = \frac{\sum_{S=1}^{N} z_{rsk}}{N} \tag{7}$$

where $Z_{rsk}(t)$ is the average z score level for the *r*-th ROIs, in the *s*-th subject, performing the *k*-th task.

Often, due to the experimental design adopted, EEG data were gathered from the same population during the performance of different behavioral tasks. In this case it can be of interest to analyze if the levels of the variable considered for the characterization of brain activity differ between tasks. In order to explore these hypothetical differences, we can use the properties of the computed z scores over the employed ROIs. In fact, due to the additive properties of the z score, it is possible to analyze if the changes of such variable between the different experimental tasks is statistically significant. The quantitative measure of the contrast between tasks 1 and 2 in the analysed population for the *i*-th BA is obtained as follows:

$$zdiff_r(t) = z_{r1}(t) - z_{r2}(t) \tag{8}$$

where $z_{i1}(z_{i2})$ is the average z score level for the *r*-th ROI during the task 1 (2), $zdiff_r(t)$ is the z score level of the difference of statistical activations for the *r*-th ROI between the task 1 and 2. If such value is over the threshold level, we can conclude that the *r*-th ROI presents variation of the analysed variable that are not due to the random fluctuation of the noise but are relative to the differences of the task performed.

2.7. From the estimation of cortical activity to the estimation of cortical connectivity

For each time point of the recorded EEG we solved the linear inverse problem, estimated the magnitude for each one of the thousand dipoles used for cortical modelling. Then, we computed the average of the magnitude of such dipoles in each ROI considered, for each time point considered. The resulting cortical waveforms, one for each predefined ROI, were then processed for the estimation of cortical connectivity by using the Directed Transfer Function [Belger et al., 1998]. The DTF is a full multivariate spectral measure, used to determine the directed influences between any given pair of signals in a multivariate data set. Let be X a set of EEG measurement from *k* channels at time *t*: $\underline{X} = [X_1(t), X_2(t), \ldots, X_k(t)]^T$, and suppose that X is adequately described by the following MVAR process:

$$\underline{X} = \sum_{i=1}^{p} -\underline{A}(i)\underline{X}(t\text{-}i) + \underline{E}(t) \tag{9}$$

which is equal to:

$$\sum_{i=0}^{p} \underline{A}(i)\underline{X}(t\text{-}i) = \underline{E}(t) \tag{10}$$

where E(t) is the vector of multivariate zero-mean uncorrelated white noise process, $A_1, A_2, \ldots A_p$ are the matrices of model coefficients and *p* is the model order. In order to investigate the spectral properties of the examined process, this equation is transformed to the frequency domain as follows:

$$A(f)\,X(f) = E(f) \tag{11}$$

where A(f) is the Fourier transform of the A(i) process. The Fourier transformed equation could read as

$$X(f) = A^{-1}(f)\,E(f) = H(f)\,E(f) \tag{12}$$

where H(f) is the transfer matrix of the system, whose element Hij represents the connection between j-th input and i-th output of the system. The spectral matrix of the process can be written as:

$$S(f)=X(f)\,X(f)^{*}=H(f)V\,H(f)^{*} \tag{13}$$

where V is the spectral matrix of the white noise input. The DTF from channel j to i , representing the causal influence from j to i, is defined as:

$$\theta_{ij}^{2}(f) = |H_{ij}(f)|^{2} \tag{14}$$

In order to be able to compare the results obtained for data strings with different power spectra, a normalization is performed by dividing each element by the squared sums of all elements of the relevant row, thus obtaining the *normalized DTF* [Kaminski and Blinowska, 1991]:

$$\gamma_{ij}^{2}(f) = \frac{|H_{ij}(f)|^{2}}{\sum_{m=1}^{k} |H_{im}(f)|^{2}} \tag{15}$$

which expresses *the ratio of the influence of channel j to channel i with respect to the influence of all other channels on i.*

3. Results

Subjects were exposed to the STM and NSTM tasks while they are under the EEG recording device. All the data in this section are relative to the time-varying spectral changes in different frequency bands during the delay period. The Fig. 3 (first column from the left) presents two estimated cortical distributions, obtained by the solution of the linear inverse problem in the spectral domain associated with the gathered EEG data. The figure presents the grand average data of the EEG recorded population relative to the variation of cortical current density power in the theta frequency band.

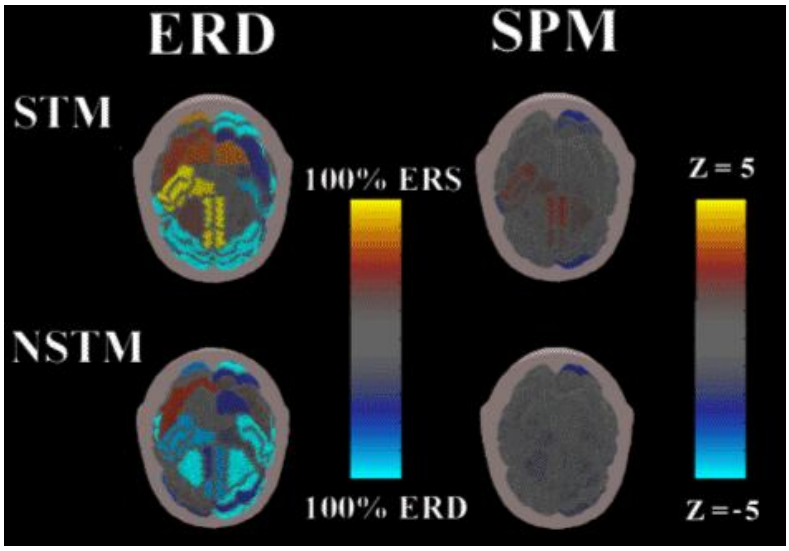

Figure 3. The first column left: Estimated cortical distributions, obtained by the solution of the linear inverse problem in the spectral domain associated with the gathered EEG data for the Short Time Memory (STM) and No Short Time Memory (NSTM). The figure presents the grand average data of the EEG recorded population relative to the variation of cortical current density power in the theta frequency band. Increasing values of spectral power with respect to the baseline period (ERS) are represented from yellow to red hues, while the decreasing values of spectral power (ERD) are coded from the dark to the light blue. The upper cortical distribution is relative to the STM task while the bottom one presents data estimated during the NSTM task. Spectral maps are relative to the time period of 1.5 seconds from the beginning of the delay period. The head is seen from above, nose down, left ear at the right of the visualized head.

Increasing values of spectral power with respect to the baseline period (ERS) are represented from yellow to red hues, while the decreasing values of spectral power (ERD) are coded from the dark to the light blue. The upper cortical distribution is relative to the STM task while the bottom one presents data estimated during the NSTM task. Spectral maps are relative to the time period of 1.5 seconds from the beginning of the delay period. The head is seen from above, nose down, left ear at the right of the visualized head. It is worth of note that during the STM task, there is a large ERS in theta band in the right and left parietal cortical areas, together with a synchronization occurring over the mesial and right premotor cortical areas.

Furthermore, a large bilateral frontal reduction of spectral power (ERD) also occurred as indicated by the blue regions over the cortical map. The NSTM task presents a different pattern of ERD and ERS with respect to the STM task. The grand averaged EEG data returned a modest ERS phenomena in the right parietal areas, together with a large bilateral ERD in frontomesial cortical areas. An interesting question is if such variation of spectral power with respect to the baseline period (the ERS and ERD) in the theta band is statistically significant or are only due to the noise fluctuations. The answer to this question is presented in the second column from the left of the Fig. 3, that shows the distribution of the statistical z scores associated to the variations of the cortical spectral power in each one of the ROIs analysed. In particular, if the power spectra during the delay period is superior to the power spectra computed during the baseline for the analysed ROI, a positive z score is obtained. Furthermore, if the z score exceeds the threshold for the statistical significance required the ROI analysed was coded with a hue from yellow to red (in the present case up to a value of z equals to 5, that it is associated to a statistical significance of $p<10^{-5}$). Instead, a decrement of spectral power in a particular ROI is statistically significant if the associated negative value of the z score is lower than the required threshold. In that case, the ROI was coded with a hue from dark to the light blue (z = -5). If the spectral power increase or decrease in the analysed ROI does not reach the threshold of the statistical significance, the ROI presents the grey color. The upper map of the right column of Fig.3 shows the grand average significance probability map for the STM task. It is worth of note the presence of a large statistically significant increase in the power spectra of the right premotor and the mesial cortical areas, coded in the red color. Of interest also a statistically significant decrease of spectral power in the theta band for the left frontal areas, coded in blue. The SPM associated with the grand average data for the NSTM task in the same frequency band is presented in the bottom map of Fig. 3, right column. In such map few cortical areas present variations of spectral power not due to the chance alone. In particular, the left frontal cortical areas showed a significant decrease in spectral power in the theta band during the NSTM task.

The application of the presented methodologies to the long-term memory task has produced the results listed in the figure 4. In this figure the Significance Parametric Mapping is presented for the grand average of all the subjects. The head is seen from above, the nose at the bottom, left ear at the right of the each head. The colour bar has the same significance described in Figure 3, i.e the z score that exceeds the threshold for the statistical significance required is coded with a hue from yellow to red (in the present case up to a value of z equals to 5, that it is associated to a statistical significance of $p<10^{-5}$), while decrement of spectral power in a particular ROI statistically significant are presented with a negative value of the z score coded with a hue from dark to the light blue (z = -5). It is interesting to note that in the theta band during the encoding time period, the data from the analyzed population in the theta band present and increased spectral activity (when compared to the rest state) located in the dorsolateral prefrontal areas (coded in the dark red), while the left prefrontal areas presents a decrement of the spectral power (when compared to the rest state) coded with the blue hues. A large increase of spectral power in the same band is also presented in the visual areas (red hues) while for the time period from 1500 to 3500 ms after the stimulus presentation a decrease of the spectral power in the theta band in the parietal areas is observed bilaterally.

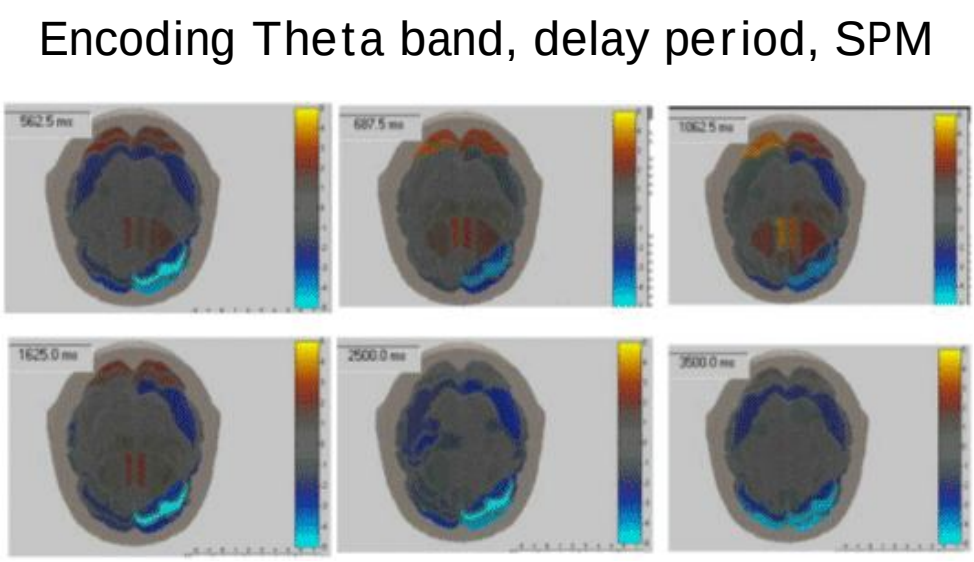

Figure 4. In this figure the Significance Parametric Mapping (SPM) is presented for the grand average of all the subjects that were subjected to the Long-Term Memory task, in the part of the Encoding of pictures. The SPM data presented are relative to the time period from about 500 ms to 3500 ms after the stimulus presentation and are referred to the theta frequency band. The head is seen from above, the nose at the bottom, left ear at the right of each head. The colour bar has the same significance described in the figure 3, i.e the z score that exceeds the threshold for the statistical significance required is coded with a hue from yellow to red (in the present case up to a value of z equals to 5, that it is associated to a statistical significance of $p<10^{-5}$), while decrement of spectral power in a particular ROI statistically significant are presented with a negative value of the z score coded with a hue from dark to the light blue (z = -5).

The estimation of the functional connectivity patterns from the above mentioned set of high-resolution EEG data was performed by the application of the DTF tool to the cortical waveforms estimated in the different ROIs considered. The network for the functional connectivity during in the theta band for the encoding-retrieval task, for the grand-average data of all the subjected analyzed is presented in the figure 5.

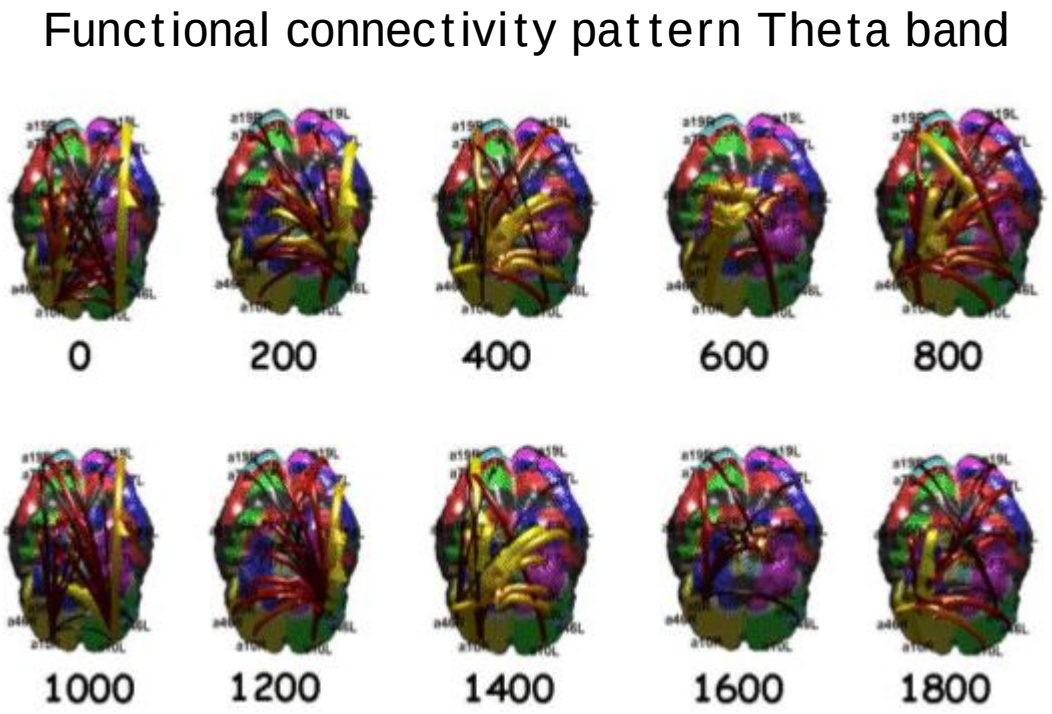

Figure 5. Sequence of functional connectivity patterns estimated by using the DTF on the grand average data for the population performing the Encoding long-term memory task. The connectivity has been computed in the theta frequency band. The cortex is seen from above, nose at the bottom, left ear to the right. The number under each map represents the ms from the stimulus presentation (see Fig. 2 for the task description). Labels on the maps code the ROIs interested in the analysis, the label R means right cortex, the label L mean left cortex. Then, A19L means Brodmann area 19 in the left hemisphere.. A functional link between two ROI is represented as an arrow, with a size and color according to the intensity of the causality flows between the two regions. The lighter the color of the arrow the stronger is the connection estimated from the ROIs. Only the statistically significant link at p<0,001 between cortical ROIs are represented here.

It is worth to note that only the statistically significant link at p<0,001 between cortical ROIs are represented here. We noted a precise directed flow of information from the prefrontal cortical areas toward the parietal and the occipital areas during the time period from the stimulus presentation up to 2. sec after. Such flow as estimated by the statistically significant connections from DTF is coded with yellow and light red arrows of appreciable size, departing from the Brodmann areas 10 and 9 directed toward the Brodmann areas 5 and 7, as well as toward the Brodmann area 19.

4. Discussion

4.1 Methodological considerations

What is often missing in EEG linear inverse solutions is the level of reliability of the solution itself. Not all modeled sources have the same degree of sensitivity to measurement noise, so we cannot say whether a source has a high strength because it is the most probable source of that potential distribution, or just because that source well accounts for the noise superimposed to the potential. Even in the ideal case of absence of noise, some sources seem more inclined to explain a large set of data, just because of their geometrical properties (i.e. sources positioned on a cortical girus, rather than deep in a sulcus). A statistical approach to the problem and a measure of the signal to noise ratio in the modeled cortical activity are then required.

In this study the cortical activity has been estimated by non-invasive EEG recording with the use of a quasi-realistic head model and linear inverse procedure. The head model used allows us to express brain activity in terms of Broadmann and Tailarach coordinates, that improves the capability to replicate results obtained with EEG recordings between different research groups. Furthermore, it alleviates the need to use individual MRIs of the experimental subjects, since they are not always available. The results of the application of the methodology proposed in the present study were reported at the ROI level instead of the level of each one of the three thousand cortical dipoles used as a source model. An ROI–dependent type of result expression such as the one used in our study has been chosen due to our interest in the reported efficacy of the estimation process at this still acceptable spatial scale

The interest in the approach presented here regards the extension of the DSPM techniques proposed by Dale and coworkers [Dale et al., 2000] to the frequency domain and in the possibility to further exploit this approach by applying contrast statistical techniques normally used in the fMRI field. It is already accepted that the estimation of current densities with the weighted minimum norm procedure from the EEG recordings can return an accurate picture of the underlying cortical activation at a moderate spatial scale [Babiloni et al., 2001; Dale et al., 1993; Grave de Peralta et al., 1999]. In this context, the use of DSPM and the related contrast techniques (z score differences between the STM and NSTM or ENC-RET tasks) provided useful insights on the phenomena studied besides the analysis of topographic distribution at the cortical level.

4.2 Short-Term Memory

Animal studies and human neuroimaging studies indicate that tasks requiring short-term memory activate a functional network linking regions of the prefrontal cortex with posterior association cortices [Belger et al., 1998; Chafee and Goldman-Rakic, 1998; Friedman and Goldman-Rakic, 1994]. Activation of this network can also be characterized by measurements of neuroelectric activity recorded on the scalp. It is of interest that recent studies have indicated that an enhancement in the power spectra in theta frequency band of EEG signal over midline frontal region of the during short-term memory tasks [Gevins et al., 1997; Gevins et al., 1998]. Enhancement of the frontal midline theta rhythm has been noted in a variety of tasks that require sustained focused attention [Gevins et al., 1997;Gevins et al., 1998]. Current evidence suggests that this signal is generated in the anterior cingulate cortex [Gevins et al., 1998], an important component of an anterior attentional network critical to the performance of complex cognitive tasks [Posner and Petersen, 1990]. The results we obtained with the DSPM techniques extended to the frequency domain can be framed in the previously described context. The centro mesial activation related to the power spectral increase in theta frequency bands has been obtained in contrast with the same experimental paradigm but without the memory task. This increase in spectral activity only holds during the delay period, while in the remaining time periods there are no significant differences between memory and non short-term memory tasks.

4.3 Encoding Retrieval Memory task

Positron emission tomography (PET), functional magnetic resonance imaging (fMRI), and event-related potential (ERP) studies have shown that, in healthy young individuals, long-term episodic memory is associated with “activation” of discrete frontal neuronal networks [Fletcher et al.,2001; Buckner and Wheeler 2000]. In particular, different aspects of the memory performance are represented in right and left prefrontal areas [Fletcher et al., 2001], which cooperate with medial temporal lobe structures for the retrieval of both verbal and non-verbal information [Buckner and Wheeler 2000]. For example, a focal “activation” of right prefrontal cortex and bilateral mediotemporal regions (i.e. parahippocampal) during the encoding phase predicts a successful recognition of visual stimuli in a later retrieval phase. The presented results allowed evaluation of the main brain rhythms of both frontal and parietal areas during the ENC and RET phases. The working hypothesis was that the brain rhythmicity represents a neural substrate of the hemispherical functional asymmetry as predicted in literature for these tasks [Tulving et al., 1994; Nyberg et al., 1996; Lepage et al., 2000].

Compared to the encoding condition, the retrieval condition (not showed here) was characterized by a posterior theta event-related synchronization and a stronger high alpha (10-12 Hz) event-related desynchronization. These results are globally in line with previous evidence [Klimesch et al. 1999] showing that theta and upper alpha rhythms are sensitive to semantic long-term memory processes and retrieval processes, possibly as a reflection of the gating oscillatory activity within thalamo-cortical (alpha) and hippocampo-cortical (theta) feedback loops. Furthermore, previous studies showed that theta and alpha rhythms are widely distributed rhythms over both hemispheres, especially with engaging cognitive demands involving working memory, focused attention, and semantic categorization [Klimesch et al.1999].

The use of the estimation of the cortical flow by using the DTF tool is able to return information about the dynamical link between ROIs during a particular task. This information is of great importance in the neuroscience, since often it is not sufficient to know where an increase of cortical activity occurs but event which are the network of cortical areas that support a particular cognitive task. The use of tools like DTF or even the Partial Directed Coherence [Baccalà and Sameshima, 2001] could return this estimation by using the high-resolution EEG recordings associated with the geometrical accurate representation of the cortical surface for the population analysed. By using these advanced computational tools, namely the high-resolution EEG and the estimation of cortical activity and connectivity by the techniques above description, the analysis of the time behaviour of the cortical activity can be performed with an accuracy never reached before by using the standard EEG measurements.

Acknowledgements

Authors thanks dr. Marco Crocenzi for the help in the editing of this manuscript

5. References

Anourova I, Nikouline VV, Ilmoniemi RJ, Hotta J, Aronen HJ, Carlson S. Evidence for dissociation of spatial and nonspatial auditory information processing. *Neuroimage*. 2001; 1268-77.

Astolfi L., Cincotti F, Babiloni C., Carducci F., Basilisco A, Rossini PM, Salinari S., Mattia D., Cerutti S, Ben Dayan D , Ding L., Ni Y, He B. and Babiloni F. Estimation Of The Cortical Connectivity By High-Resolution EEG And Structural Equation Modeling: Simulations And Application To Finger Tapping Data, *IEEE Trans Biomed Eng*. 2005a May;52(5):757-68.

Astolfi L., Cincotti F, Mattia D., Babiloni C., Carducci F., Basilisco A, Rossini PM, Salinari S.,. Ding L., Ni Y, He B. and Babiloni F., Assessing Cortical Functional Connectivity By Linear Inverse Estimation And Directed Transfer Function: Simulations And Application To Real Data, *Clin Neurophysiol. 2005b Apr;116(4):920-32*.

Babiloni F., Carducci F., Cincotti F., Del Gratta C., Pizzella V., Romani G.L., Rossini P.M., Tecchio F., and Babiloni C., 2001, Linear inverse source estimate of combined EEG and MEG data related to voluntary movements, *Human Brain Mapping*, 14(4):197-210.

Babiloni F, Cincotti F, Babiloni C., Carducci F., Basilisco A, Rossini PM, Mattia D., Astolfi L., Ding L., Ni Y, Cheng K, Christine K, Sweeney J , He B., Estimation of the cortical functional connectivity with the multimodal integration of high resolution EEG and fMRI data by Directed Transfer Function, *Neuroimage*, 2005a Jan 1;24(1):118-31.

Baccalà L.A., Sameshima K, Partial Directed Coherence: a new concept in neural structure determination. *Biol. Cybern.*, 84: 463-474, 2001.

Baillet S. and Garnero L., A bayesian framework to introducing anatomo-functional priors in the EEG/MEG inverse problem., *IEEE Trans. Biomed. Eng.* 44:374-85, 1997.

Baillet S., Garnero L., Marin G. and Hugonin P., 1999, Combined MEG and EEG source imaging by minimization of mutual information, *IEEE Trans. Biom. Eng.*. 46:522-34, 1999.

Belger A., A. Puce J.H., Krystal J.C., Gore P. Goldman-Rakic G., McCarthy. Dissociation of mnemonic and perceptual processes spatial and nonspatial working memory using fMRI, *Hum .Brain Mapp*. 6 (1998) 14–32.

Bokura H., Yamaguchi S. and Kobayashi S. Electrophysiological correlates for response inhibition in a Go/NoGo task, *Clinical Neurophysiology* 112 (2001) 2224–2232.

Buckner RL., Wheeler ME. The cognitive neuroscience of remembering. Nat Rev Neurosci. 2(9): 624-34, 2000.

Brovelli A., Ding M., Ledberg A., Chen Y., Nakamura R., Bressler SL., Beta oscillations in a large-scale sensorimotor cortical network: directional influences revealed by Granger causality. *Proc Natl Acad Sci U S A.* Jun 29;101(26):9849-54, 2004.

Buchel C., Friston KJ., Modulation of connectivity in visual pathways by attention: cortical interactions evaluated with structural equation modelling and fMRI. *Cereb Cortex* 7(8):768-78, 1997.

Chafee M.V, Goldman-Rakic P.S., Matching patterns of activity in primate prefrontal area 8a and parietal area 7ip neurons during a spatial working memory task, *J. Neurophysiol*. 79:2919, 1998.

Clifford Carter G. Coherence and time delay estimation. *Proc.I.E.E.E*. 75, 236– 255, 1987.

Dale A.M. and Sereno M., Improved localization of cortical activity by combining EEG anf MEG with MRI cortical surface reconstruction: a linear approach, *J. Cognitive Neuroscience*, 5: 162-76, 1993.

Dale A., Liu A., Fischl B., Buckner R., Belliveau J. W., Lewine J. and Halgren, E., Dynamic Statistical Parametric Mapping: Combining fMRI and MEG for High-Resolution Imaging of Cortical Activity, *Neuron* 26:55-67, 2000.

Fallgatter AJ, Strik WK. The NoGo-anteriorization as a neurophysiological standard-index for cognitive response control. *Int J Psychophysiol*. Jun;32(3):233-8, 1999.

Fletcher P.C., Henson R.N.A. Frontal lobes and human memory. Insights from functional neuroimaging. Brain. 124: 849-881, 2001.

Friedman H., Goldman-Rakic P.S., Coactivation of prefrontal cortex and inferior parietal cortex in working memory tasks revealed by 2DG functional mapping in the Rhesus monkey, *J. Neurosci*. 14:2775–2788, 1994.

Gevins A.S., Cutillo B.A., Bressler S.L., Morgan N.H., White R.M., Illes J., Greer D.S. Event-related covariances during a bimanual visuomotor task. II. Preparation and feedback. *Electroencephalogr. Clin. Neurophysiol.* 74, 147–160, 1989.

>Gevins A., Smith M.E., McEvoy L., Yu D., High resolution EEG mapping of cortical activation related to working memory: effects of difficulty, type of processing, and practice, *Cereb. Cortex* 7, 374–385, 1997.

Gevins A., Smith M.E., Leong H., McEvoy L., Whitfield S., Du R., Rush G. Monitoring working memory load during computer-based tasks with EEG pattern recognition methods, *Hum. Fact.* 40:79-91, 1998.

Grave de Peralta R. and Gonzalez Andino S. Distributed source models: standard solutions and new developments. In Analysis of neurophysiological brain functioning, In: Uhl C, ed. New York: Springer Verlag), pp. 176-201, (1998).

Grave de Peralta Menendez R., Gonzalez Andino SL. Distributed source models: standard solutions and new developments. In: Uhl, C. (ed): Analysis of neurophysiological brain functioning. *Springer Verlag*, pp.176-201, 1999.

Gross J., Timmermann L., Kujala J., Salmelin R., Schnitzler A. Properties of MEG tomographic maps obtained with spatial filtering. *NeuroImage* 19:1329-1336, 2003.

Horwitz B. The elusive concept of brain connectivity. *Neuroimage* 19:466-470, 2003.

Inouye T., Iyama A., Shinosaki K., Toi S. and Matsumoto, Y. Inter-site EEG relationships before widespread epileptiform discharges. *Int. J. Neurosci.* 82, pp. 143–153, 1995.

Klimesch W. EEG alpha and theta oscillations reflect cognitive and memory performance: a review and analysis.*Brain Res Brain Res Rev*. Apr;29(2-3):169-95, 1999.

Lee L., Harrison LM., Mechelli A. The functional brain connectivity workshop: report and commentary, *Neuroimage* 19, 457-465, 2003.

Lepage M., Ghaffar O., Nyberg L., Tulving, E. Prefrontal cortex and episodic memory retrieval mode. *Proc. Natl. Acad. Sci*. 97, 506-511, 2000.

McIntosh AR., Gonzalez-Lima F. Structural equation modelling and its application to network analysis in functional brain imaging. *Hum.Brain Mapp*. 2p. 2-22, 1994.

Nyberg L., McIntosh AR., Cabeza R., Habib R., Houle S., Tulving E. General and specific brain regions involved in encoding and retrieval of events: what, where, and when. *Proc Natl Acad Sci U S A.* 93(20): 11280-5, 1996.

Nunez PL. Neocortical dynamics and human EEG rhythms, *Oxford University Press*, New York 1995.

Okada YC., Salenius S. Roles of attention, memory, and motor preparation in modulating human brain activity in a spatial working memory task. *Cereb Cortex*. Jan-Feb;8(1):80-96, 1998.

Otsubo H., Ochi A., Elliott I., Chuang SH., Rutka JT., Jay V., Aung M., Sobel DF., Snead OC. MEG predicts epileptic zone in lesional extrahippocampal epilepsy: 12 pediatric surgery cases. *Epilepsia*. Dec;42(12):1523-30, 2001.

Pascual-Marqui RD. Reply to comments by Hämäläinen, Ilmoniemi and Nunez. *ISBET Newsletter* 6: 16-28, 1995.

Phillips JW., Leahy R., Mosher JC. Imaging neural activity using MEG and EEG. *IEEE Eng in Med and Biol Mag* 16:34-41, 1997.

Posner M.E., Peterson S.E., The attentional system of the human brain, *Annu. Rev. Neurosci*. 13:25–42, 1990.

Pfurtscheller, G. and Aranibar, A. Event-related cortical desynchronization detected by power measurements of scalp EEG. *Electroenceph clin Neurophysiol* 42, pp. 817–826, 1977.

Pfurtscheller G., Lopes da Silva FH. Event-related EEG/MEG synchronization and desynchronization: basic principles. *Clin Neurophysiol*. Nov;110(11):1842-57, 1999.

Salmelin R., Forss N., Knuutila J., Hari R. Bilateral activation of the human somatomotor cortex by distal hand movements. *Electroenceph clin Neurophysiol* 95:444-452, 1995.

Scherg M., von Cramon D. and Elton M. "Brain-stem auditory-evoked potentials in post-comatose patients after severe closed head trauma", *J Neurol* 231(1): 1-5, 1984.

Stam CJ., Breakspear M., van Cappellen van Walsum AM., van Dijk BW. Nonlinear synchronization in EEG and whole head MEG recordings of healthy subjects. *Hum. Brain Mapp*. 19(2), 63– 78, 2003.

Stam CJ., van Dijk BW. Synchronization likelihood: an unbiased measure of generalized synchronization in multivariate data sets. *Physica*, D 163, 236– 251, 2002.

Stenbacka L., Vanni S., Uutela K., Hari R. Comparison of minimum current estimate and dipole modeling in the analysis of simulated activity in the human visual cortices. *Neuroimage*. Aug;16(4):936-43, 2002.

Tononi G., Sporns O., Edelman GM. A measure for brain complexity: relating functional segregation and integration in the nervous system. *Proc. Natl. Acad. Sci. U. S. A.* 91, 5033– 5037, 1994.

Torquati K., Pizzella V., Della Penna S., Franciotti R., Babiloni C., Rossini PM., Romani GL. Comparison between SI and SII responses as a function of stimulus intensity., *Neuroreport*. May 7;13(6):813-9, 2002.

Tulving E., Kapur S., Craik FI., Moscovitch M., Houle S. Hemispheric encoding/retrieval asymmetry in episodic memory: positron emission tomography findings.*Proc Natl Acad Sci USA*. 91: 2016-20, 1994.

Urbano A., Babiloni C., Onorati P., Babiloni F. Dynamic functional coupling of high resolution EEG potentials related to unilateral internally triggered one-digit movements. *Electroencephalogr Clin Neurophysiol*. 106(6):477-87, 1998.

Uutela K., Hamalainen M., Somersalo E. Visualization of magnetoencephalographic data using minimum current estimates. *Neuroimage*. Aug;10(2):173-80, 1999.

Zar H. Biostatistical analysis. Prentice-Hall, New York, 1984.